Large scale synthesis of ordered silver nanoparticles for superhydrophobic and anti-icing application

A. Safaee, D. K. Sarkar and M. Farzaneh

Canada Research Chair on Atmospheric Icing Engineering of Power Networks and
Industrial Chair on Atmospheric Icing of Power Network Equipment,
Université du Québec à Chicoutimi, Canada G7H 2B1

ABSTRACT

An optimized reduction of silver ions in presence of ethylene glycol (EG) and polyvinylpyrrolidone (PVP) produced colloidal silver nanoparticles in the solution. This colloidal solution has been spin-coated on glass substrates, annealed, and finally coated with thin films of polytetrafluoroethylene (PTFE) by plasma sputtering. AFM studies show that the size of the as-deposited silver nanoparticles is ~60 nm and it increases with the duration of annealing. However, UV-Vis investigation reveals that particle size initially increases with the time of annealing then starts reducing. This contradictory observation is due to the oxidation of silver and the present investigation confirms that the larger particles seen on AFM images are actually silver oxides rather than silver *per se*. Silver nanoparticles annealed at different duration were coated with PTFE. The resulting samples showed a decrease in hydrophobicity with annealing time. This observation is explained by assuming that the spherical silver nanoparticles are partially embedded onto the smooth surface used as substrate.

Keywords: colloidal silver nanoparticles, spin coating, AFM, hydrophobicity.

1 INTRODUCTION

Metallic nanoparticles have gained much interest because of their special mechanical, optical, electrical, and magnetic properties [1-3]. It is not only the size of the particles that influences the characteristics of a material but also their morphology and relative spatial arrangement of the nanoparticles may be of great importance [4,5,6]. In general, metal nanoparticles can be prepared and stabilized not only by physical techniques [7] but also by several chemical methods such as photochemical [8,9] electrochemical [10,11] and chemical reductions [12,13].

Generally, metal atoms formed by wet methods tend to join to form oligomers, which in turns grow into larger clusters and finally into precipitates [14]. However, this process may be prevented if a cluster stabilizer is added. Several mechanisms for the formation of metal nanoparticles with a stabilizer have been reported; these vary according to the reaction materials and the reduction methods [15]. In order to keep the silver colloid within the nanometer range, polyvinylpyrrolidone (PVP) was used almost exclusively as the protective agent during synthesis either in ethylene glycol or aqueous solution [16]. Carotenuto *et al.* [17] used sonic activation at room temperature and also obtained silver nanoparticles after a 24-hourreaction time. Zhang *et al.* synthesized silver nanoparticles stabilized with polyvinylpyrrolidone (PVP) by using hydrazine as a reducing agent [18]. In the ethylene glycol or polyol process, the alcohol served both as solvent and reducing agent for the silver ions.

Hydrophobicity is currently the focus of considerable research. Wettability is an important characteristic of solid surfaces and is controlled by the chemical composition and the geometrical structure of the surfaces [19,20]. The main idea is to develop an outer shell of material with very low surface energy. Since the interactions between water drops and solid are limited to the outermost layer of surface, it is possible to cover the material with some passivating film [21]. Drops of water on smooth hydrophobic surfaces do not usually form angles to the solid surface which are greater than 120°. The addition of roughness to the surface can increase the contact angle without altering its chemistry [22]. Many strategies are being currently investigated to control structure, dimensions, and regularity of the patterns that can be obtained [23]. Often such surfaces can be prepared in such a way that water drops simply roll off if they are tilted even slightly. Rolling drops have been observed to remove contamination, and such super-hydrophobic surfaces with low contact angle hysteresis are referred to as self-cleaning. Accordingly, various phenomena such as the adherence of snow or raindrops, oxidation, and friction drag are expected to be inhibited or reduced on such surfaces [24].

2 EXPERIMENTAL

Two separate solutions were prepared using 1.1 gm $AgNO_3$ (Alfa Aesar) in 20 ml ethylene glycol (EMD) and 1.7 gm polyvinylpyrrolidone (M.W. 44000 from BDH) in 10 ml ethylene glycol, respectively. A 5 ml ethylene glycol was heated at 160°C for 20 minutes, while stirring at 400 rpm. While continuing the stirring and heating, 10 ml of each

previously prepared solutions are simultaneously injected into this hot solution within 10 minutes. This mixture was further stirred continuously for more than 45 minutes at the same temperature. During this period, ethylene glycol reduces silver ions to silver atoms forming colloidal silver nanoparticles in the solution. The prepared colloidal solution was spin-coated on glass and silicon surfaces. These spin-coated samples were annealed at 300 °C for various time periods, and then coated with polytetrafluoroethylene (PTFE) thin films using plasma sputtering. The surface morphology of the samples was investigated using a Digital Instruments Nanoscope III atomic force microscope (AFM) UV-Vis spectroscopy (Agilent company model 8453) was used to monitor the presence of silver nanoparticles both in the solution and on the glass surfaces. Equilibrium contact angle (CA) measurements were made using a Krüss DSA100 goniometer.

3 RESULTS AND DISCUSSIONS

Figure 1 shows the UV-Vis spectrum of silver nanoparticles in the solution, which is confirmed by the appearance of a prominent surface plasmon resonance absorption peak at around 405 nm as was reported in the literature [25]. The solution with nanoparticles in suspension was spin-coated onto glass and silicon substrates to bring the silver nanoparticles onto the surfaces.

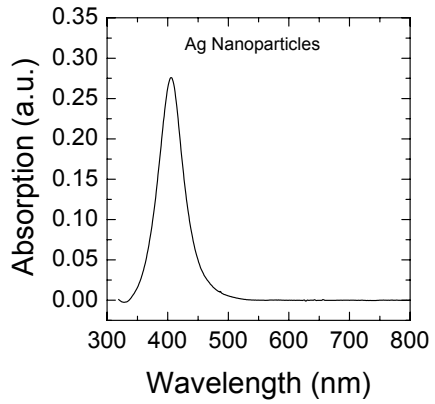

Figure 1: The UV-Vis absorption in colloidal silver nanoparticles solution.

AFM was used to study the morphology of the annealed films both on glass and silicon surfaces. AFM images in four different times of the annealing process have are in figure 2. Figure 2 (a) shows the AFM image of as-deposited silver nanoparticles having size of ~60 nm and an average roughness of ~2.1 nm. The size of the particles increased to 115 nm with a increase in roughness to 3.8 nm after annealing of 15 minutes at 300 °C. Particle size further increased to ~204 nm with roughness 5.4 nm when annealed for 40 minutes. A sharp increase in particles size to ~350 nm and in roughness to ~25 nm was observed when the film has been annealed for 60 minutes. Largely, the AFM study confirms that particle size grows as a function of annealing time. It is obvious from the images that nearby particles agglomerate to form particles of larger size and lower density. This agglomeration process clearly affects the morphology of the surface as shown figure 2.

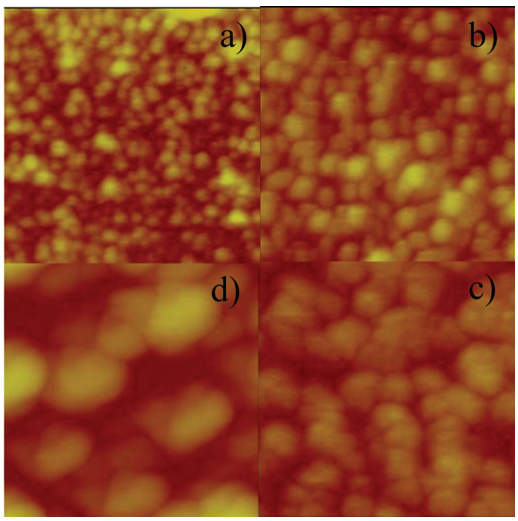

Figure 2: AFM images of samples annealed at 300 °C for different time with a scan size of 1 μm×1 μm: (a) as-deposited, (b) 10 min, (c) 40 min, and (d) 60 min.

Figure 3 shows the UV-Vis spectra of spin-coated samples on glass substrates. A distinct plasmon resonance absorption peak is observed around 430 nm with an area of 0.2 under the peak for the as-deposited sample. The initially colorless glass sample turns to yellow as a result of the absorption of blue light by the silver nanoparticles. The effect of annealing time at 300 °C on the growth of the silver nanoparticles is shown in figure 3. The peak position shifts to 450 nm after a 10-minute annealing time and the area under the peak is enhanced to 11. This red-shift of the absorption peak position and increase in peak intensity are due to the increase in size of the silver nanoparticles [26], which is complemented with the AFM results. The peak position does not change substantially for the sample annealed for 15 minutes; even though area under the curve is increased to 18. The sample annealed for 25 minutes shows a strong peak as compared to the other samples and is very asymmetric. The peak has been deconvoluted into two Gaussian peaks, the main one centered at 455 nm with an area of 43.6 and the other one at 561 nm with an area of only 12.3, showing that this sample is composed of two different sizes of silver nanoparticles. The appearance of an absorption peak at higher wavelengths indicates that the particles are larger than those associated with an absorption peak at lower wavelengths [26- 28]. The AFM image of this

sample is also in agreement with this result (picture not shown). Further increase of annealing time to 40 minutes, reduces the area under the curve to 25 and the main absorption peak position shifts a lower wavelength of 431 nm while the other peak shifts to 530 nm after deconvolution. This reduction in peak area is related to the loss in the number of silver nanoparticles and the blue-shift is correlated with the reduction of the size of the nanoparticles [26].

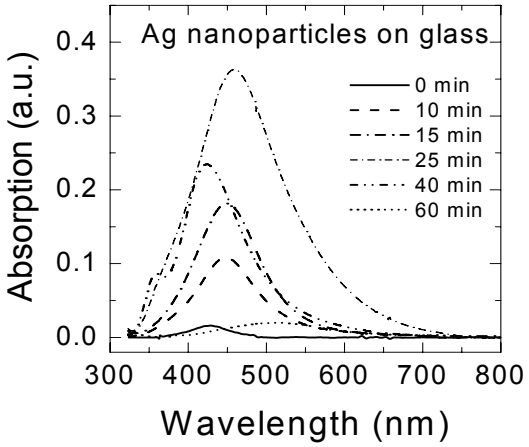

Figure 3: The UV-Vis absorption spectroscopy of silver nanoparticles annealed at 300 ^{o}C for different annealing time.

The simultaneous reduction of in size and number of nanoparticles can be related to their oxidation. It is easier to oxidize a nanoparticle as compared to bulk since the nanoparticles possess more surface atoms than mass-equivalent bulk. Though UV-Vis indicates that the silver nanoparticles reduce in size at that time of annealing, AFM shows that average particle size actually increases to 200 nm as depicted in figure 2. In order to understand this apparent contradiction, we must realize that AFM determines only the topography of a surface independently of the presence of oxide or metal. Thus, we can interpret this UV-Vis observation by assuming the presence of a shell of silver oxides around silver nanoparticles which effectively shows nanoparticles of larger size, as seen in the AFM images. After annealing time of 60 minutes, the smaller particles are completely oxidized and the size of the larger particles is further reduced UV-Vis spectrum of this sample shows a small peak centered at 515 nm with an area of only 3. The presence of the strong peak at around 450 nm is totally vanished due to the complete oxidation of the small particles following that absorption. Conversely, AFM shows that the size of the particles has increased to ~350 nm as a result of oxidation.

Figure 4 shows the behavior of the contact angle of water (CA) on the samples coated with a thin PTFE film by plasma sputtering. CA for both as-deposited and 10-minute annealing time samples are observed to be 132^{o}, while the PTFE coated polished silicon (or glass) samples exhibits a CA of 110^{o}. Therefore, it is clear that the CA of the PTFE coated samples has been increased by 22$^{o.}$ This is due to the presence of nanoparticles on the surfaces. However, CA of the samples annealed for 60 minutes before PTFE coating reduces to 122^{o}.

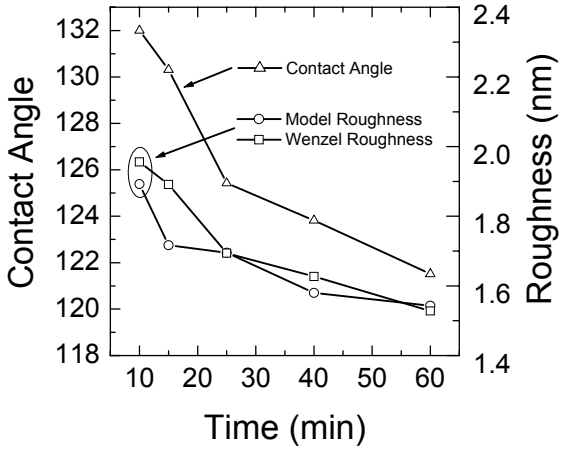

Figure 4: Contact angle of water and roughness with annealing time.

From figure 4, it is observed that the CA of PTFE coated samples decreases with annealing time of those samples before PTFE coating. Although obtained AFM rms roughness increases with annealing time, the CA decreases in our observation. It is reported in the literature that the CA is proportional to the AFM rms roughness [29]. However, contradictory results are also reported in the literatures [29]. As water sticks to those surfaces, it can be assumed that a water drop on the PTFE/silver oxide/silver nanosurface follows the Wenzel model [30]. According to this model, the so-called critical contact angle of water on a nanosurface (θ_c) is related to the contact angle of water on a smooth surface (θ) by the following equation:

$$\cos\theta_c = r\cos\theta \qquad (1)$$

where r is the ratio of the total area of the nanosurface to the area of the smooth surface. The different r values for the samples annealed at different times have been calculated using the Eq. (1) utilizing their corresponding θ_c values presented in figure 4 for a θ of 110^{o} for PTFE films on smooth surface. The calculated r values have also been plotted with annealing time in figure 4. It is obvious that the r values decreases with the increase in annealing time. A

similar *r* factor has been calculated from the AFM images. The average size and spacing between two nanoparticles have been determined from the AFM section analysis and is used in our model to explain the CA behavior. In this model, partially embedded spherical (not a hemisphererical) nanoparticles on a smooth surface is assumed to calculate the *r* factor. The detailed mathematical analysis of this model will be discussed elsewhere. It is clear from figure 4 that the calculated *r* factors using our model are similar to the corresponding *r* values obtained using Wenzel equation. Though the rms roughness determined from AFM increases with the increase of annealing time, the *r* factor decreases and so does the contact angle.

4 CONCLUSION

Colloidal silver nanoparticles were produced in solution from $AgNO_3$ in the presence of ethylene glycol and were spin-coated on glass and silicon surfaces. The plasmon resonance absorption peaks of UV-Vis spectra were observed in the range of 430-560 nm for the nanoparticles covered spin-coated samples after annealing at 300 ^{o}C for different time periods. The silver nanoparticles were oxidized through a long time of annealing and covered with a shell of silver oxide. AFM showed an increase in nanoparticle size from 60 nm to 300 nm due to the increase in annealing time. PTFE coated silver nanoparticles dispersed samples reduce their hydrophobicity with the increase of their annealing time prior to PTFE coating. The observed results with regards to hydrophobicity are explained by assuming that the spherical particles are partially embedded on a smooth surface and by calculating the *r* factor related to the gain of surface area due to the presence of nanoparticles.

5 ACKNOWLEDGMENT

This work was carried out within the framework of the NSERC/Hydro- Québec/UQAC Industrial Chair on Atmospheric Icing of Power Network Equipment (CIGELE) at the University of Québec in Chicoutimi. The authors would like to thank all the sponsors of the project.

REFERENCES

[1] P. V Kamat, J. Phys. Chem. B, 106, 7729, 2002.
[2] M. Valden, X. Lai; D.W. Goodman, Science, 281, 1647, 1998.
[3] C. Binns, Surf. Sci. Rep., 1, 44, 2001.
[4] M.A. El-Sayed, Acc. Chem. Res. 34, 257, 2001.
[5] J.F. Sampaio, K.C. Beverly, J.R. Heath, J. Phys. Chem. B 105, 8797, 2001.
[6] S. Henrichs, C. Collier, R. Saykally, Y. Shen, J. R. Heath, J. Am. Chem. Soc., 122, 4077, 2000.
[7] G. Mitrikas, C.C. Trapalis, N. Boukos, V. Psyharis, L. Astrakas, G. Kordas, J. Non-CrystallineSolids 224, 17, 1998.
[8] R. He, X. Qian, J. Yin, Z. Zhu, J. Mater. Chem., 12, 3783, 2002.
[9] F. Mafune, J.Y. Kohno, Y. Takeda, T. Kondow, J. Phys. Chem. B, 104, 8333, 2000.
[10] J.J. Zhu, S.W. Liu, O. Palchik, Y. Koltypin, A. Gedanken, Langmuir, 16, 6396, 2000.
[11] Y.Y. Yu, S.S. Chang, C.L. Lee, C.R.C. Wang, J. Phys.Chem. B, 101, 6661, 1997.
[12] I. Pastoriza-Santos, L.M. Liz-Marzan, Langmuir, 15, 948, 1999.
[13] W. Yu, Y. Wang, H. Liu, W. Zheng, J. Mol. Catal. A, 112, 105, 1996.
[14] K. Mallick, Z.L.Wang, T. Pal, J. Photochem. Photobiol. A, 140,75, 2001.
[15] A. Henglein, M. Giersig, J. Phys. Chem. B 103, 9533, 1999.
[16] K.S. Chou, Y.S. Lai, Materials Chemistry and Physics, 83, 82, 2004.
[17] G. Carotenuto, G.P. Pepe, L. Nicolais, Eur. Phys. J. B, 16, 11, 2000.
[18] Z. Zhang, B. Zhao, L. Hu, J. Solid State Chem. 121, 105, 1996.
[19] L. Feng, S. Li, Y. Li, H. Li, L. Zhang, J. Zhai,; Y. Song, B. Liu, L. Jiang, D. Zhu, Adv. Mater. 14, 1857, 2002.
[20] Z.Z. Gu, H. Uetsuka, K. Takahashi, R. Nakajima, H. Onishi, A. Fujishima, O. Sato, Angew. Chem., Int. Ed., 42, 894, 2003.
[21] S.A. Kulinich, M. Farzaneh, Vacuum, 79, 255, 2005
[22] Z. Yoshimitsu, A. Nakajima, T. Watanabe, H. Hashimoto, Langmuir, 18, 5818, 2002.
[23] W. Chen, A.Y. Fadeev, M.Ch. Hsieh, D. Oner, J. Youngblood, T.J. McCarthy, Langmuir, 15, 3395, 1999.
[24] T. Kako, A. Nakajima, H. Irie, Z. Kato, Z. Uematsu, T. Watanabe, Hashimoto, Journal of Materials Science, 39, 547, 2004
[25] M. Andersson, J.S. Pedersen, A.E.C. Palmqvist, Langmuir, 21, 11387, 2005.
[26] H. Bao, G. Chumanov, R. Czerw, D.L. Carroll, S.H. Foulger, Colloid Polym Sci, 283, 653, 2005
[27] K. Lance Kelly, E. Coronado, L. L. Zhao, G.C. Schatz, J. Phys. Chem. B, 107, 668, 2003.
[28] S. Link, M.A. El-Sayed, Int. Reviews in Physical Chmistry, 19, 409, 2000.
[29] G. Cicala, A. Milella, F. Palumbo, F. Favia, R. d'Agostino, Diamond and related Materials, 12, 2020, 2003.
[30] R.N. Wenzel, J. Phys. Colloid Chem., 53, 1466, 1949.